ACCURATE BER / SER ANALYSIS AND PERFORMANCE OF DIFFERENT MODULATION SCHEMES OVER WIRELESS FADING CHANNELS

Anam Ilyas, Ejaz A. Ansari, Saleem Akhtar
Department of Electrical Engineering, COMSATS Institute of Information Technology (CIIT),
1.5 km Defense Road, off Raiwind Road, Lahore - Pakistan.
anamilyas@ciitlahore.edu.pk, dransari@ciitlahore.edu.pk, sakhtar@ciitlahore.edu.pk

ABSTRACT**:** *This paper derives accurate analytical expressions for bit-error (BER) and symbol-error (SER) rate of different modulation schemes such as binary phase shift keying (B-PSK), binary frequency shift keying (B-FSK), quadrature phase shift keying (Q-PSK), 8-phase shift keying (8-PSK) and 16-quadrature amplitude modulation (16-QAM) over Nakagami-m fading channels respectively. These analytical expressions are extremely useful for evaluating the system's performance without carrying out time consuming simulations. Subsequently, we verify our derived closed form expressions for Rayleigh fading channels by setting the value of Nakagami fading parameter, m equal to 1. We further validate our derived theoretical results by performing Monte Carlo Simulations of the System Model. The performances of different modulation schemes under Nakagami-m fading channels are analyzed using the average bit / symbol error probability. Furthermore, we also make the performance comparison of modulation schemes under Nakagami-m fading channel with other fading channels such as Rician and Rayleigh and show that the performance of the system is better in case of Nakagami-m fading channels as compared to other fading channels.*

Key Words*: bit-error rate, communication, fading channels, performance results, symbol-error rate.*

1 INTRODUCTION

In wireless communications, the environment between the transmitter and the receiver is not always ideal, i.e., the line of sight (LoS) is not always present during the propagation of the signal. There are many propagation paths including both LoS and non LoS which are available in wireless communication due to the obstruction with the walls, houses, forest, buildings, towers and mountains. Thus, the signal that propagates through the wireless channel not only degrades with additive white Gaussian noise (AWGN) but also due to the multi-path propagation. The receivers often do not receive the exact transmitted signal in such an environment. The received signals are thus the superposition of multiple copies of the transmitted signal each propagates through different path and experiences different attenuation while travelling from the sending end to the receiving end [1]. This can result either in constructive or destructive interference of the signal which is known as fading.

Fading channels in wireless communication systems arise as a result of multi-path propagation for the transmitted signal. Fading usually modeled as a "*Random Process*" may vary with time, frequency and geographical position. Rayleigh fading simulates that statistical model in which the signal passing through the transmission medium will fade according to a Rayleigh distribution and is applicable only when there is no LoS path present between the two communication points [2]. If LoS propagation path is present between the two points, then Rician fading is more appropriately to apply and the signal passing through the transmission medium will fade according to the Rician distribution. The Nakagami-*m* distribution [3] has been used and employed as another useful and important model for characterizing the amplitude of the fading channel. It is more general and flexible distribution in the sense that it takes care of many statistical conditions by changing the value of the Nakagami parameter, *m*. The smaller the value of *m*, the more severe is the amount of fading on the received signal which further increases the chances of making the probability of error more by the receiver. We can simulate various distributions by adopting a certain value of the parameter, *m*. For example, Nakagami-*m* distribution behaves like the Rayleigh distribution for $m = 1$. The other two special cases are one-sided Gaussian distribution and non-fading AWGN which are modeled by setting $m = 0.5$ and $m = \infty$, respectively [4].

2 RELATED WORK

Mohammad Riaz Ahmed and MD.Asaduzzaman [2] compared the symbol error probability (SEP) for different *M*-ary modulation schemes over Rician fading channels. They performed the exact analysis of SEP using maximal ratio combining (*MRC*) scheme with '*N*' branch receive diversity when the receiver knows the channel state information (*CSI*). Lindsey [5] derived the performance characteristics for coherent and non-coherent multi-receivers. The crux of this study illustrates that fast fading introduces additional noise components and multichannel reception which is more effective when applied on the random multichannel. Jonqyuin Sun and Irving S.Reed [6] derived analytical expressions for average error rate of *M*-DPSK, coherent *M*-PSK, and non-coherent *M*-FSK over slow flat Rician fading channels. A.Annamalai *et al.* [7] derived BER/SER of different modulation schemes with/without diversity using characteristic function (CHF) method in a fading environment. Jack H.Winters, *et al.* [8] considered Nakagami- *m* fading channels to derive SEP of different modulation schemes using *MRC* technique. Chandra [9] derived the closed form series solution for *B*-PSK, *B*-FSK, *DB*-PSK and *M*-QAM over Rician fading channels. In this study, the performances of different frequency bands are also observed through experimental measurements in case of terrestrial mobile systems and indoor wireless channels. Ejaz A. Ansari and Nandana Rajatheva [10] performed the precise error-rate analysis of

multiple-input multiple-output (MIMO) based orthogonal frequency division multiplexing (OFDM) systems for *M*-ary modulation schemes over Nakagami-*m* fading channels using orthogonal space time block codes (OSTBCs). They used probability density function (PDF) approach in deriving the accurate analytical expressions for SER. A. Annamalai, and C. Tellambura derived new analytical formulas of error probabilities in Rayleigh and Nakagami- *m* fading channels for single and multichannel communications [11]. A. Annamalai, *et al.* computed precise integral expressions for the symbol-error rate (SER) of *M*-QAM utilizing *L*-fold antenna diversity on Nakagami-*m* fading channel [12]. Marvin K. Simon and Mohamed-Slim Alouini [13] presented a unified approach towards the performance analysis of digital communication over generalized fading channels. Alouini and Goldsmith [14] used MGF approach for computing the error performance of coherent modulation schemes over Nakagami-*m* fading channels. However, average symbol error probability method is used in this paper for evaluating the system performance over Nakagami-*m* fading channels.

The contributions of this paper are the following: We first derive the accurate analytical expressions of average bit and symbol error probability for different modulation schemes (B-PSK, B-FSK, Q-PSK, 8-PSK, 4-QAM and 16-QAM (square constellations) under Nakagami-*m* fading channels. We then verify our computed theoretical results for Rayleigh fading channels by setting *m = 1* in the derived analytical results. Furthermore, we validate our derived theoretical results through Monte Carlo simulations. Finally, we do the performance comparison of modulation schemes under Nakagami-*m* fading channel with other fading channels such as Rician and Rayleigh fading channels.

This paper is organized as follows: Section 3 briefly describes the system model. In Section 4, we derive the general expression of average SEP for the performance analysis of different modulation schemes. Reduction of theoretical results to Rayleigh fading is discussed in section 5. In Section 6, we discuss our numerical results. Finally, in section 7, the important points are summarized in the form of conclusion.

3 DERIVATION OF ANALYTICAL RESULTS

It is a well known fact that the transmitted signal gets degraded due to fading and the presence of the noise introduced by the channel. Therefore, the signal obtained at the receiving end known as received signal, *r*(*t*) which equals as [15]

$$r(t) = \alpha\, e^{j\phi}\, s(t) + n(t) \tag{1}$$

where $s(t)$ is the transmitted signal, $r(t)$ is the received signal, α is the amplitude and ϕ is the phase and *n(t)* is the additive Gaussian noise component.

In the received signal, amplitude of the instantaneous attenuation α may belong to a different distribution such as Rayleigh, Rician or Nakagami-*m*. The received signal is then demodulated and detected. Number of errors is calculated by comparing the transmitted and received signal bits. Finally the probability of error is found by dividing the no of errors to the total number of bits transmitted.

In this paper, we mainly consider the Nakagami-*m* distribution. The envelope of the received signal is Nakagami-*m* distributed and its PDF is given by [16]

$$p(\alpha) = \frac{2}{\Gamma(m)}\left(\frac{m}{\Omega}\right)^{m} \alpha^{2m-1} \exp\left(\frac{-m\alpha^{2}}{\Omega}\right) \tag{2}$$

where *m* is Nakagami fading parameter, Γ(.) is the Gamma function and Ω represents an instantaneous power, i.e. $\Omega = E[X^2]$. The instantaneous signal to noise ratio (SNR) per bit/symbol is the random variable related to signal's amplitude as $\gamma = (E_b/N_o)\alpha^2$ where E_b is average bit energy of the transmitted signal, N_o is the power spectral density of noise and α is the attenuation factor due to fading. The PDF of the instantaneous SNR under Nakagami-*m* distribution is given by [17]

$$p(\gamma) = \beta \gamma^{m-1} e^{-m\left(\gamma/\bar{\gamma}\right)} \tag{3}$$

where $\beta = m^{m} \Big/ \left(\Gamma(m) \times \bar{\gamma}^{m}\right)$ and $\bar{\gamma}$ is the mean value of the instantaneous SNR per symbol/bit which can be written as

$$\bar{\gamma} = E[\gamma] = E\left[\left(\frac{E_b}{N_o}\right)\alpha^2\right] = \frac{E_b}{N_o} E[\alpha^2]$$

4 PERFORMANCE ANALYSIS

Wireless communication system is the world's most famous system which is widely spread all over the globe. It has acquired high data rates and has shown better voice quality as compared to the other communication system channels. The system performance can be measured through outage probability, average symbol error probability and average signal to noise ratio.

The PDF based approach is exploited in this paper to compute the average bit/symbol error probability. Using [18]

$$P_e = \int_0^{\infty} P_e(\gamma) p(\gamma) d\gamma \tag{4}$$

where $P_e(\gamma)$ is the conditional symbol error probability (SEP) over AWGN channel and $p(\gamma)$ is the PDF of the fading channel. Using general expression of conditional SEP over AWGN similar to the form of [9]

$$P_e(\gamma) = k_1 Q\left(\sqrt{k\gamma}\right) + k_2 Q^{2}\left(\sqrt{k\gamma}\right) \tag{5}$$

where k_1, k_2 and k are the constants which are listed in Table I for different modulation schemes and Q is the standard Marcum-Q function.

We can use (2.3-18) [19], (7.1.2) and (7.1.21) [20] for converting Q- function into complementary error function and further for simplifying the complementary error function respectively. Substituting (5) in (4), the average bit/symbol error probability, after some manipulation and simplification, becomes

$$P_e = \int_0^{\infty} \Big[\frac{k_1}{2} + \frac{k_2}{4} - \frac{2}{\sqrt{\pi}}\left(\frac{k_1}{2} + \frac{k_2}{2}\right)\sqrt{\frac{k}{2}}\sqrt{\gamma}\exp\left(-\frac{k}{2}\gamma\right){}_1F_1\left(1, \frac{3}{2}, \frac{k}{2}\gamma\right) + \frac{k_2 k\gamma}{2\pi}\exp(-k\gamma)\,{}_1F_1\left(1, \frac{3}{2}, \frac{k}{2}\gamma\right)^2\Big] p(\gamma) d\gamma \tag{6}$$

Using linearity, (6) can further be written in compact form as

$$P_e = \frac{k_1}{2} + \frac{k_2}{4} - \frac{2}{\sqrt{\pi}}\left(\frac{k_1}{2} + \frac{k_2}{2}\right)\sqrt{\frac{k}{2}}A + \frac{k_2 k}{2\pi}B \qquad (7)$$

where

$$A = \int_0^\infty \sqrt{\gamma}\exp\left(-\frac{k}{2}\gamma\right){}_1F_1\left(1,\frac{3}{2},\frac{k}{2}\gamma\right)p(\gamma)d\gamma$$

and

$$B = \int_0^\infty \gamma\exp(-k\gamma)\left({}_1F_1\left(1,\frac{3}{2},\frac{k}{2}\gamma\right)\right)^2 p(\gamma)d\gamma \qquad (8)$$

Now substitute (3) in (8), the constants A and B become

$$A = \int_0^\infty \sqrt{\gamma}\exp\left(-\frac{k}{2}\gamma\right){}_1F_1\left(1,\frac{3}{2},\frac{k}{2}\gamma\right)\beta\gamma^{m-1}\exp\left(-m\frac{\gamma}{\bar{\gamma}}\right)d\gamma$$

and

$$B = \int_0^\infty \gamma\exp(-k\gamma)\left({}_1F_1\left(1,\frac{3}{2},\frac{k}{2}\gamma\right)\right)^2\beta\gamma^{m-1}\exp\left(-m\frac{\gamma}{\bar{\gamma}}\right)d\gamma \qquad (9)$$

TABLE I
COEFFICIENTS FOR DIFFERENT MODULATION SCHEMES

Modulation Schemes	k	k_1	k_2
B-PSK	2	1	0
B-FSK	1	1	0
Q-PSK	2	2	-1
8-PSK	0.876	2	0
16-QAM	0.8	3	-2.25

First taking A for simplification from (9), we may write it as

$$A = \beta\int_0^\infty \gamma^{m-\frac{1}{2}}\exp\left(-\gamma\left(\frac{k}{2}+\frac{m}{\bar{\gamma}}\right)\right){}_1F_1\left(1,\frac{3}{2},\frac{k}{2}\gamma\right)d\gamma \qquad (10)$$

where ${}_1F_1$ is the confluent hypergeometric function as defined in [20]. By using the expression of β defined in (3) and the relations (15.3.4) [20] and (7.621.4) [21], the closed form for A can thus be found as

$$A = \frac{\Gamma\left(m+\frac{1}{2}\right)}{\Gamma(m)}\sqrt{\frac{\bar{\gamma}}{(k/2)\bar{\gamma}+m}}\left(\frac{m}{(k/2)\bar{\gamma}+m}\right)^{m-1}{}_2F_1\left(1,-m+1,\frac{3}{2},\frac{-(k/2)\bar{\gamma}}{m}\right) \qquad (11)$$

where ${}_2F_1$ is the Gauss hypergeometric function as defined in [21]. Now taking B for simplification from (9), we have

$$B = \beta\int_0^\infty \gamma^m\exp\left(-\gamma\left(k+\frac{m}{\bar{\gamma}}\right)\right)\left({}_1F_1\left(1,\frac{3}{2},\frac{k}{2}\gamma\right)\right)^2 d\gamma \qquad (12)$$

With the help of [9], B can further be written in the form of

$$B = \beta\frac{\Gamma(m+1)}{\left(k+\frac{m}{\bar{\gamma}}\right)^{m+1}}F_2\left(m+1,1,1,\frac{3}{2},\frac{3}{2},\frac{(k/2)\bar{\gamma}}{k\bar{\gamma}+m},\frac{(k/2)\bar{\gamma}}{k\bar{\gamma}+m}\right) \qquad (13)$$

where F_2 is Appell hypergeometric function in two variables as defined in [21]. Now using the relation from [22], the closed form for B can also be found as

$$B = \frac{\Gamma(m+1)}{\Gamma(m)}\frac{1}{m}\left(\frac{\bar{\gamma}}{k\bar{\gamma}+m}\right)\sum_{j=0}^{m-1}\left(\frac{m}{k\bar{\gamma}+m}\right)^j{}_2F_1\left(1,j+1,\frac{3}{2},\frac{(k/2)\bar{\gamma}}{k\bar{\gamma}+m}\right) \qquad (14)$$

Using the results obtained for constants A and B in eqs. (11) and (14), final expression for the probability of error given in eq. (7) can now easily be obtained.

5 REDUCTION OF THEORETICAL RESULTS TO RAYLEIGH FADING CHANNEL

We can reduce our theoretical results obtained in eq. (7) to Rayleigh fading channels by substituting $m = 1$ in eqs. (11) and (14). Under this condition,

$$\Gamma\left(m+\frac{1}{2}\right) = \frac{\sqrt{\pi}}{2} = 0.8862,\ \Gamma(m) = 1,\ \Gamma(m+1) = 1$$

and

$${}_2F_1\left(1,-m+1,\frac{3}{2},\frac{-(k/2)\bar{\gamma}}{m}\right) = 1$$

$$P_e = \frac{k_1}{2} + \frac{k_2}{4} - \frac{2}{\sqrt{\pi}}\left(\frac{k_1}{2} + \frac{k_2}{2}\right)\sqrt{\frac{k}{2}}A + \frac{k_2 k}{2\pi}B \qquad (15)$$

where

$$A = \frac{\sqrt{\pi}}{2}\sqrt{\frac{\bar{\gamma}}{(k/2)\bar{\gamma}+1}}$$

and

$$B = \left(\frac{\bar{\gamma}}{k\bar{\gamma}+1}\right){}_2F_1\left(1,1,\frac{3}{2},\frac{(k/2)\bar{\gamma}}{k\bar{\gamma}+1}\right)$$

Using (15.3.4) and (15.1.5) [20], B can also be written in the form of arctan as

$$B = \left(\frac{\bar{\gamma}}{k\bar{\gamma}+1}\right)\frac{k\bar{\gamma}+1}{(k/2)\bar{\gamma}+1}\sqrt{\frac{(k/2)\bar{\gamma}+1}{(k/2)\bar{\gamma}}}\arctan\left(\sqrt{\frac{(k/2)\bar{\gamma}}{(k/2)\bar{\gamma}+1}}\right)$$

Final expression becomes

$$P_e = \frac{k_1}{2} + \frac{k_2}{4} - \frac{2}{\sqrt{\pi}}\left(\frac{k_1}{2} + \frac{k_2}{2}\right)\sqrt{\frac{k}{2}}A + \frac{k_2 k}{2\pi}B \qquad (16)$$

where

$$A = \frac{\sqrt{\pi}}{2}\sqrt{\frac{\bar{\gamma}}{(k/2)\bar{\gamma}+1}}$$

and

$$B = \left(\frac{\bar{\gamma}}{k\bar{\gamma}+1}\right)\frac{k\bar{\gamma}+1}{(k/2)\bar{\gamma}+1}\sqrt{\frac{(k/2)\bar{\gamma}+1}{(k/2)\bar{\gamma}}}\arctan\left(\sqrt{\frac{(k/2)\bar{\gamma}}{(k/2)\bar{\gamma}+1}}\right)$$

These results are the same as have been reported in [5], [9] and [19].

6 SIMULATION RESULTS

Fig. 1 illustrates block diagram of the system model. The parameters used in the simulation are also described in Table II. Source generator in the system model generates a stream of random bits as 0 or 1. These bits then enter into the modulator block where the random bits are modulated. The modulated signal passes through the channel which induces a Gaussian noise into it, i.e., in the modulated signal. We use Monte Carlo simulation to validate our analytical results. In simulation 100,000 – 500,000 bits are passed through the system and 20 max. runs are considered for calculating the BEP/SEP for each value of SNR.

Finally, we get the signal at the receiving end known as received signal. The probability of error is computed by dividing the no. of errors to the total no. of bits sent. The no. of bits and maximum runs are very important parameters in the simulation model. As we increase the value of these parameters, the simulation results get better and exactly approach to the analytical results.

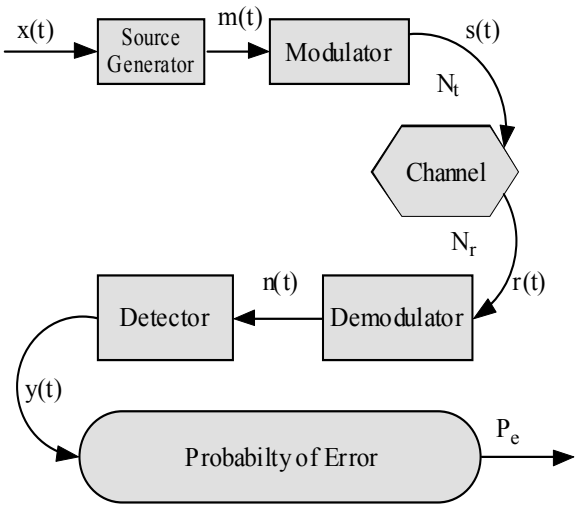

Figure 1. System model block diagram for simulation

TABLE II
PARAMETERS USED IN THE SYSTEM MODEL

Simulation Parameters	Values Used
Nakagami fading parameter, *m*	1, 2, 2.28, 3, 3.77, 4, 5 and 9
Modulation Schemes	B-PSK, B-FSK, Q-PSK, 4-QAM, 8-PSK, & 16-PSK
Number of transmit and receive antenna, N_t & N_r used	1,1

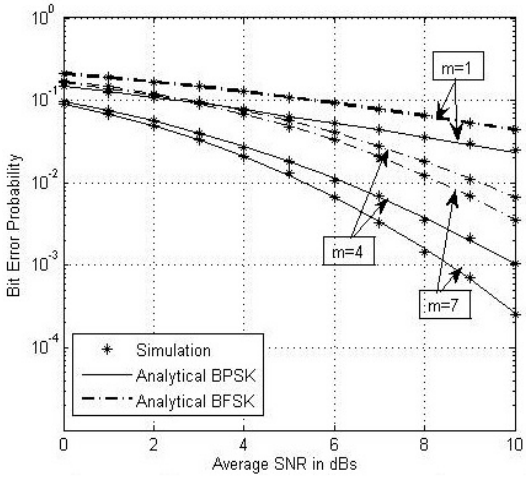

Figure 2. Comparison of Analytical and Simulation Results for B-PSK and B-FSK schemes over Nakagami‘*m* fading channel (*m* = 1,4 and 7)

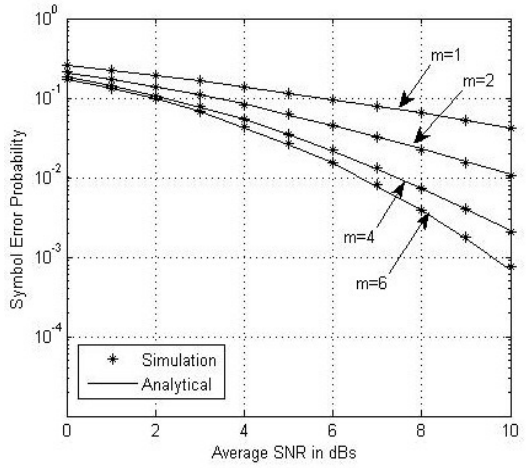

Figure 3. Comparison of Analytical and Simulation Results for Q-PSK scheme over Nakagami-*m* fading channel (*m* = 1, 2, 4 and 6)

Fig. 2 depicts the performance comparison of B-PSK and B-FSK at *m* = 1, 4 and 7. These results show that system's performance gradually gets better as the value of *m* is increased. Analytical results are shown by the lines where solid line is for B-PSK and dash line is for B-FSK. It is evident from the figure that the system performs better in case of B-FSK compared to B-PSK for the same SNR value because the probability of error is better in the former case than in the later one. We also draw the simulation results represented by the symbol (*) on the same graph for comparison purpose. Fig. 2, shows that the simulation results match with our analytical results very closely and thus validates our analytical results for B-FSK and B-PSK.

Fig. 3 shows the analytical results for Q-PSK or 4-QAM under Nakagami-*m* fading channel including the Rayleigh fading channel. The values of '*m*' used are 1,2, 4 and 6 respectively. The results again demonstrate that the performance of the system gets better and better as the value of '*m*' is increased correspondingly. Moreover, we again draw the simulation results represented by the symbol (*) on

the same graph for comparison purpose. It is clearly seen that our analytical results are very much supported by Monte Carlo simulation results.

Fig. 4 illustrates our analytical results for 8-PSK under Nakagami-*m* fading channel. The values of '*m*' used are 1, 5 and 9 respectively. It is obvious from this figure that the system shows an improved performance with the increase in the value of '*m*'. Simulation results are also plotted using the symbol (*) on the same graph for comparison purpose. The figure shows that our analytical results are very much supported by the Monte Carlo simulation results.

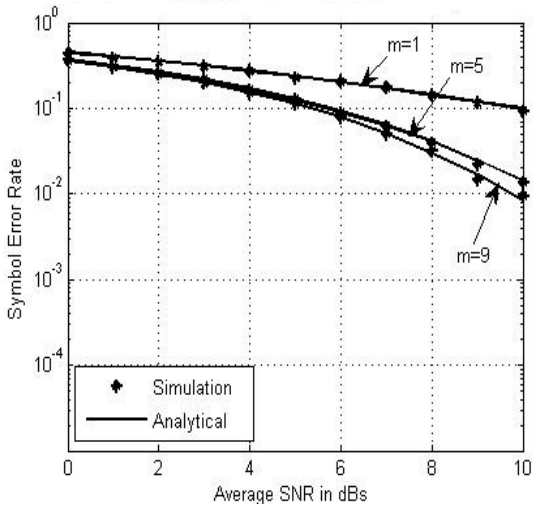

Figure 4. Comparison of Analytical and Simulation Results for 8-PSK scheme over Nakagami-*m* fading channel (*m* = 1,5 and 9)

Fig. 5 shows the comparison of our analytical results with Monte Carlo simulation results for 16-PSK under Nakagami-*m* fading channel. The values of *m* used are 1, 2, 3 and 4 for the range of average SNR from 0 to 20 dBs. Solid lines show the analytical results while simulation results are indicated on the same graph with the symbol (*). It can easily be concluded from the figure that our simulation results perfectly match with the derived analytical results.

Fig. 6 shows the comparison of our derived analytical results for 16-QAM under Nakagami-m fading channel with the simulation results. The values of the fading factor m used are 1, 2, 3 and 4 respectively. Simulation results are indicated by the symbol (*) on the same graph. The figure demonstrates that our simulation results perfectly match with the derived theoretical results.

We consider the general expression of average SEP derived in eq. (7) and further use the values of the constants from Table II according to the required modulation scheme. Fig. 7 shows performance comparison of B-PSK and B-FSK modulation schemes over Nakagami-m fading channel when m is varied from 1, 3, 5 and 7. For B-PSK values of constants are $k_1=1$, $k_2=0$, $k=2$ and for B-FSK, these are $k_1=1$, $k_2=0$, $k=1$. We already know from the literature that more the value of '*m*' the less is the amount of fading on the received signal which improves the system's performance by decreasing the probability of error. The worst case of fading in wireless communication channel is the Rayleigh fading and it is modeled by setting the value of $m = 1$.

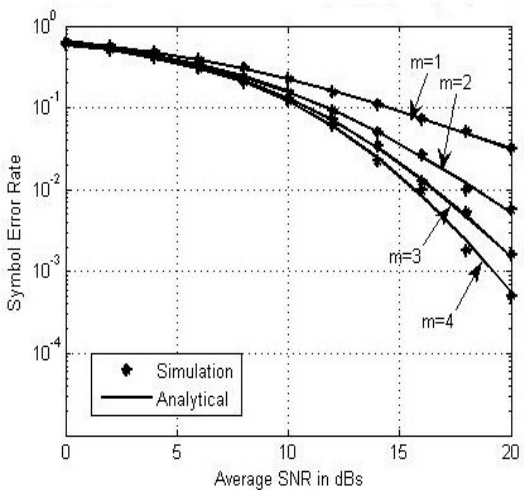

Figure 5. Comparison of Analytical and Simulation Results for 16-PSK scheme over Nakagami-m fading channel (m = 1, to 4)

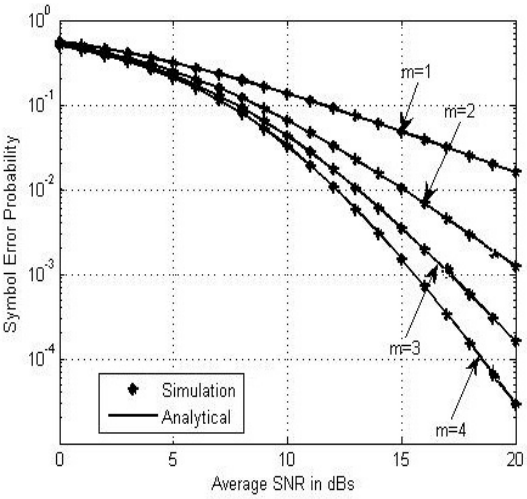

Figure 6. Comparison of Analytical and Simulation Results for 16-QAM scheme over Nakagami-*m* fading channel (*m* = 1 to 4)

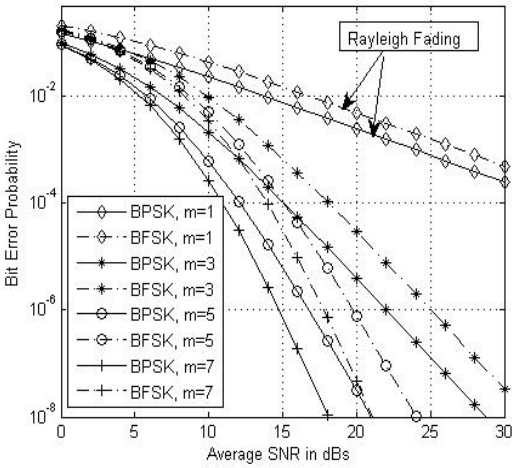

Figure 7. Average BEP versus average SNR of B-PSK and B-FSK in Nakagami-'m' fading channel for different values of fading factor, (*m* =1, 3, 5 and 7)

Fig. 8 shows the average SEP versus average SNR in dBs for Q-PSK and 4-QAM square constellation. The curves show that the system's performance remains the same for both types of constellation schemes. This is due to the fact that 4-QAM constellation is achieved from 4-PSK by simply rotating it through an angle of 45^0 in the CCW direction. The range of fading factor '*m*' used here is from 1 to 5.The figure illustrates that the performance of the system gets improved as we increase the value of '*m*' from 1 which is the worst case, i.e., the upper bound of SEP. The non-fading scenario (AWGN case) can also be represented on the same figure by

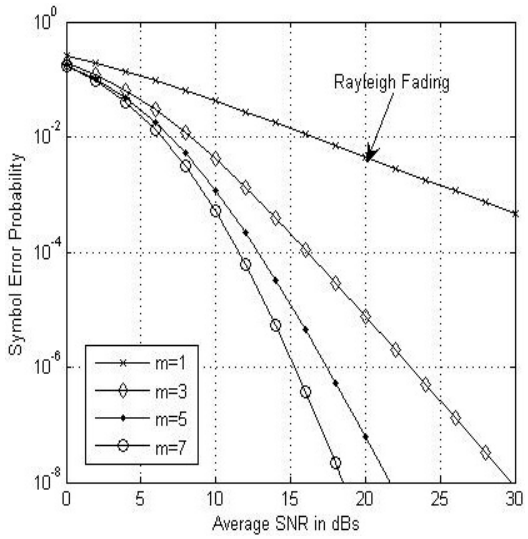

Figure 8. Average SEP versus average SNR of Q-PSK in Nakagami-*m* fading channel for different values of fading factor, (*m* = 1, 3, 5 and 7)

setting the value of m equal to ideally infinity but practically quite large in eq. (7). This will represent the lower mound of the SEP and we thus expect to have the system's performance to vary between these two extremes respectively.

Fig. 9 describes the comparison of analytical results of the 16-PSK with 16-QAM modulation schemes under Nakagami-*m* fading channel. The values of '*m*' used for this purpose are 1 to 5. These curves illustrate that the system's performance is better in case of 16- QAM than 16- PSK for the same value of '*m*' This is due to the fact that for each value of SNR, the SEP for 16-QAM is better (less) than that of 16- PSK (more).

Fig. 10 shows the performance comparison of the system in case of Rayleigh, Rician and Nakagami-m fading channels. We have considered B-PSK modulation scheme for this purpose. In this plot, we compare the performance analysis of the B-PSK under three different types of fading channels. First, we have considered Rayleigh fading channel which corresponds to $K = 0$ in Rician fading and $m = 1$ in Nakagami-m fading. This is represented in Fig. 10 by the solid line in case of $K = 0$ (Rician Fading) and by the symbol (*) for the Nakagami-m fading channel for $m = 1$. The results represented by the solid line and the stars overlap in this case as both represent the Rayleigh fading channel.

These results have already been validated in section 5. The relationship between the Rician fading factor '*K*' and the Nakagami-*m* fading factor '*m*' is

$$K = \frac{\sqrt{m^2 - m}}{m - \sqrt{m^2 - m}}, \quad m = \frac{K^2 + 2K + 1}{2K + 1} \tag{17}$$

By using the relation given in eq. (17), we compute *m* equal to 1 when $K = 0$. Similarly, when $K = 3$ then $m = 2.2857 \approx 2.29$ and likewise when $K = 6$ then $m = 3.7692 \approx 3.77$ respectively. These values are also shown in Fig. 10. When $K = 3$ in Rician fading, the curve is shown by the dash line; whereas for $m = 2.23$ in case of Nakagami-*m* fading, the curve is marked by the cross symbols. From these curves it is evident that the performance of the system is better in case

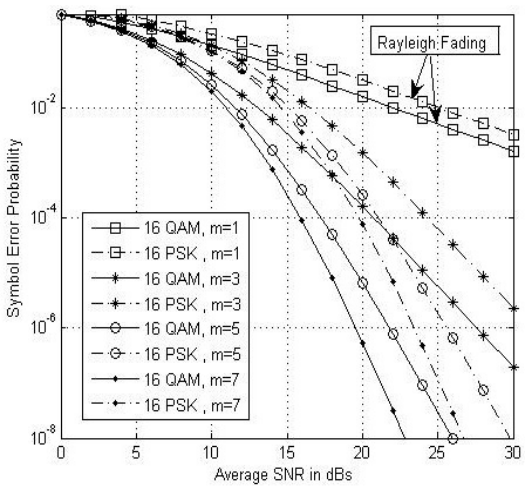

Figure 9. Average SEP versus average SNR of 16- PSK and 16-QAM in Nakagami-*m* fading channel (*m* = 1, 3, 5 and 7)

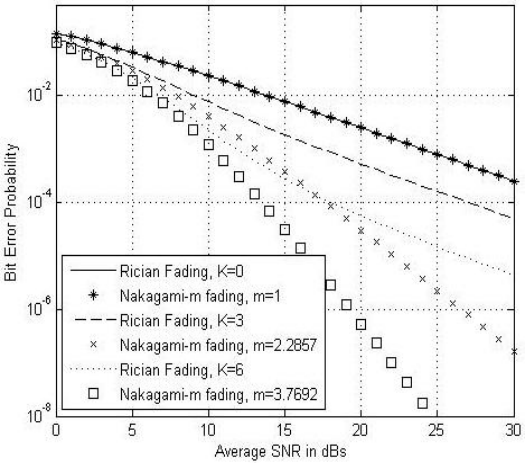

Figure 10. Performance comparison of B-PSK under Rayleigh, Rician and Nakagami-*m* fading channel

of Nakagami-*m* fading channel as compared to both Rician and Rayleigh fading channels respectively.

Fig. 11 shows the performance comparison of 8-PSK under Rayleigh, Rician and Nakagami-*m* fading channels. When the Rician fading factor $K = 0$ then Nakagami-*m* fading

factor *m = 1* and both Rician and Nakagami-*m* fading reduces to Rayleigh fading which is shown by the solid line and the line containing the symbol stars. Again from these curves it can easily be seen that the performance of the system is better in case of Nakagami-*m* fading channel as compared to both Rician and Rayleigh fading channels respectively.

Finally, Fig. 12 does the performance analysis of the 16-PSK under Rayleigh, Rician and Nakagami-*m* fading channels. We consider *K = 0, 3* and *6* for Rician fading channel; then *m = 1, 2.23* and *3.77* for Nakagami-*m* fading channel by using the relation given in eq. (17). It can also easily be concluded from these curves that the system's performance is again better for the case of Nakagami-*m* fading channel as compared to Raician and Rayleigh fading channels respectively.

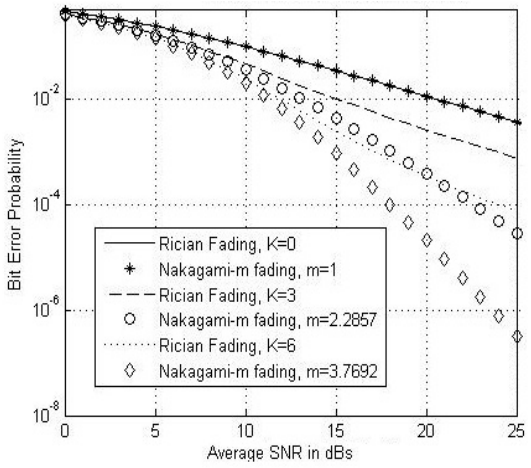

Figure 11. Performance comparison of 8-PSK under Rayleigh, Rician and Nakagami-*m* fading channel

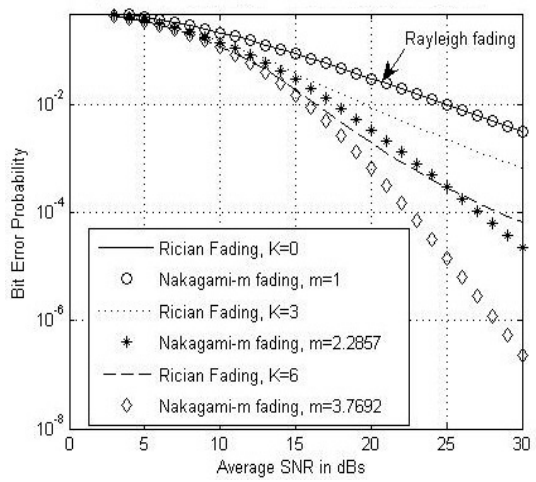

Figure 12. Performance comparison of 16-PSK under Rayleigh, Rician and Nakagami-*m* fading channel

7 CONCULUSION

In this paper, we derived the accurate analytical expressions for bit-error and symbol-error rate (BER/SER) of different modulation schemes over Nakagami-m fading channels. These theoretical expressions are extremely important for evaluating the performance of the system without carrying out time consuming simulations. The verification of derived analytical results was carried out for Rayleigh fading channels by setting the value of m equal to 1in our derived results. Monte Carlo simulation of the system model was performed to validate our theoretical results for different modulation schemes. The analysis of performance comparison of different modulation schemes under Nakagami-*m* fading channels was done using the average bit/symbol error probability. Finally, we did the performance comparison of various modulation schemes under Nakagami-*m* fading channel with other fading channels such as Rician and Rayleigh fading channels and showed that the system exhibits an improved performance in case of Nakagami-*m* fading channels as compared to other fading channels.

ACKNOWLEDGMENT

We are extremely grateful to the Department of Electrical Engineering of COMSATS Institute of Information Technology (CIIT) for carrying out this work. Moreover, we are also thankful to the anonymous reviewers for their valuable suggestions towards the improvement with respect to the quality of the paper.

REFERENCES

[1] Zhang, Q., Liu, E. and Leung, K.K, Cooperate Communication and Networking, *Cambridge University Press*, (2009).

[2] Ahmed, M. R., Ahmed, R., Robin, R. A., Asaduzzaman, Hossain, M. and Awal, A., Performance Analysis of different M-ary Modulation Techniques in Fading Channel using different diversity, *Journal of Theoretical and Applied Information Technology*, **15**(1): 23-28(2005).

[3] Du, Z., Cheng, J. and Beaulieu, N. C., Error Rate of OFDM Signals on Frequency Selective Nakagami-m Fading Channels, *IEEE Communications Society Globecom*, **6**: 3994-3998(2004).

[4] Win, M. Z., and Winters, J. H., On Maximal Ratio Combining in Correlated Nakagami Channels with Unequal Fading Parameter and SNR's among Branches: An Analytical Framework, *IEEE Wireless System*, **3**: 1058-1064 (1999).

[5] Lindsey, W. C., Error probabilities for Rican Fading Multichannel Reception of Binary and M-ary Signals, *IEEE Trans. Information Theory*, **10**: 339-350 (1964).

[6] Sun, J., and Reed, I. S., Performance of MDPSK, MPSK, and noncoherent MFSK in Wireless Rician Fading Channels, *IEEE Trans. Communications*, **47**(6): 813-816 (1999).

[7] Annamalai, A., Tellambura, C., and Bhargava, V. K., A General Method for Calculating Error Probabilities Over Fading Channels , *IEEE Trans. Communications*, **53**(5): (2005).

[8] Win, M. Z., and Chrisikos, G., MRC Performance for M-ary Modulation in Arbitrarily Correlated Nakagami Fading Channels, *IEEE Communications Letters*, **4**(10): (2000).

[9] Chandra. A., and Bose, C., Performance of Single and Multichannel Coherent Reception under Rician Fading, *Int J Wireless Inf Networks* **16**:81-90, (2009).

[10] Ansari. E. A., and Rajatheva, N., Percise SER Analysis and Performance Results of OSTBC MIMO-OFDM Systems over Uncorrelated Nakagami-m Fading Channels, *IEICE Trans. Communications*, **93**(6): (2010).

[11] Annamalai. A., and Tellambura, C., Error Rates for Nakagami-m Fading Multichannel Reception of Binary and M-ary Signals, *IEEE Trans. Communications*, **49**(1): (2001).

[12] Annamalai, A., Tellambura, C., and Bhargava, V. K., Exact Evaluation of Maximal-Ratio and Equal-GainDiversity Receivers for M-ary QAM on Nakagami Fading Channels, *IEEE Trans*. *Communications*, **47**(9): 1335-1344(1999).

[13] Simon, M. K., and Alouini, M. S., A Unified Approach to the Performance Analysis of Digital Communication over Generalized Fading Channels, *Proceedings of the IEEE*, **86**(9): 1860-1877(1998).

[14] Alouini, M. S., and Goldsmith, A. J., A Unified Approach for Calculating Errors of Linearly Modulated Signals over Generalized fading channels, *IEEE Trans. Wireless Communications*, **47**(9): 1324-1334(1998).

[15] Jafarkhani, H., Space-Time Coding (Theory and Practice), *Cambridge University Press*, (2005).

[16] Goldsmith, A., Wireless Communications, *Cambridge University Press*, (2005).

[17] Papoulis, A. and Pillai, S. U., Probability, Random Variables and Stochastic Processes, 4th ed., *Tata McGraw-Hill*, (2002).

[18] Simon, M. K. and Alouini, M. S., Digital Communication over Fading Channels, 2nd ed., *John Wiley and Sons, Hoboken, NJ*, (2005).

[19] Proakis, J. G. and Salehi, M., Digital Communications, 5th ed., *McGraw-Hill, New York*, (1995).

[20] Abramowitz, M. and Stegun, I. A., Handbook of Mathematical Functions, *Dover New York*, (1972).

[21] Gradshteyn, I. S. and Ryzhik, I. M., Table of Integrals, Series and Products, 7th ed., *Academic Press, San Diego, CA*, (2007).

[22] Falujah, I. A. and Prabhu, V. K., Performance analysis of MQAM with MRC over Nakagami-m Fading Channels, *Electronic Letters*, **42**(4): 231-233(2006).